Colloids and Surfaces A 531 (2017) 32–39

Contents lists available at ScienceDirect

Colloids and Surfaces A

journal homepage: www.elsevier.com/locate/colsurfa

Research Paper

Coalescence stability of water-in-oil drops: Effects of drop size and surfactant concentration

Nadya I. Politova[a], Slavka Tcholakova[a,*], Sonya Tsibranska[a], Nikolai D. Denkov[a], Kerstin Muelheims[b]

[a] Department of Chemical and Pharmaceutical Engineering, Faculty of Chemistry and Pharmacy, Sofia University, 1164 Sofia, Bulgaria
[b] BASF SE, 67056 Ludwigshafen, Germany

GRAPHICAL ABSTRACT

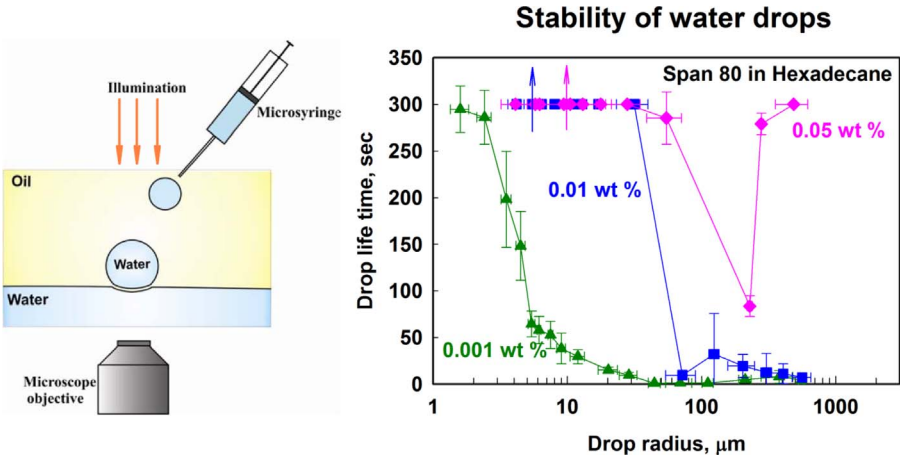

ARTICLE INFO

Keywords:
Drop coalescence
Emulsion film
Emulsion stability
Water-in-oil emulsion
Span surfactant

ABSTRACT

We study the effects of (1) drop size; (2) surfactant chain-length and concentration; and (3) viscosity of the oil phase on the stability of water drops, pressed by gravity towards planar oil-water interface. The experimental results show that at low surfactant concentrations (around and below the CMC) the drop lifetime is controlled by the drainage time of the oily film, viz. by the time for reaching the critical film thickness at which this film ruptures. The small drops coalesce before the formation of a planar film with the large interface and, as a consequence, their lifetime rapidly decreases with the increase of drop diameter. In contrast, the bigger drops coalesce after formation of a plane-parallel film and their lifetime increases with the drop diameter. Therefore, the drop lifetime passes through a minimum when varying the drop diameter. The obtained results at low surfactant concentrations and for small drops are described well by theoretical models, available in the literature. The lifetime of the respective larger drops is shorter, as compared to the theoretical predictions, due to the faster thinning of the oil films which are with uneven thickness. The increase of surfactant concentration above the CMC leads to a significant increase in the stability of the small drops. Interestingly, the stability of the intermediate in size drops remains low for all surfactants and oils studied. At higher surfactant concentrations,

* Corresponding author at: Department of Chemical and Pharmaceutical Engineering, Faculty of Chemistry and Pharmacy, Sofia University, 1 James Bourchier Ave., 1164 Sofia, Bulgaria.
E-mail addresses: SC@LCPE.UNI-SOFIA.BG, sc@dce.uni-sofia.bg (S. Tcholakova).

http://dx.doi.org/10.1016/j.colsurfa.2017.07.085
Received 15 June 2017; Received in revised form 27 July 2017; Accepted 27 July 2017
Available online 29 July 2017
0927-7757/

the stability of the large water drops increases significantly when Span 80 is used, while it remains rather low for drops stabilized by Span 20. The results obtained with single water drops are in a good agreement with the stability of the respective batch water-in-oil emulsions.

1. Introduction

The stability of oily drops [1–12] and air bubbles [13–16] in aqueous solutions is widely studied in relation to the stability of oil-in-water emulsions and foams. In the course of these studies it was found that the drop stability depends strongly on the drop size [4,5,10–12], the type and concentration of the surfactants used [1,4,10,11], the viscosity of the continuous phase [10], and the aging time for protein stabilized drops [11]. It was shown that at low surfactant concentrations, the drops are hydrodynamically stabilized and their stability depends strongly on their size [12]. When approaching large oil-water interface, the small drops coalesce before forming a plane-parallel film with the large interface, in the so-called "Taylor regime", and their lifetime rapidly decreases with increasing the drop diameter. In contrast, the bigger drops coalesce after forming a plane-parallel film with the large interface in the so-called "Reynolds regime" which results in a steady increase of their lifetime with the drop diameter [17]. As a consequence, the drops with intermediate size have the lowest stability. These theoretical predictions have been validated by experiments performed with soybean oil drops, having different diameters and placed in protein solutions with low concentration [12].

It has not been studied so far how these trends apply for the reverse system – water drops pressed by gravity against large oil-water interface. Such investigation is relevant in the context of water drop coalescence in water-in-oil (W/O) emulsions.

Only recently one study was reported on the lifetime of water drops pressed by gravity against oil-water interface, in which the effects of adsorbed microparticles and interface aging were investigated [18]. It is shown in [18] that the microparticles lead to more reproducible data for the coalescence time, showing dependence on the drop diameter and interface aging. The authors observed longer drop lifetimes with increasing the drop diameter in the presence of particles [18]. This investigation, however, is performed with rather large drops, with diameters between 1 mm and 5 mm, which are much bigger than the micrometer drops present in the most common emulsions. Thus, a study preformed in the lower range of drops sizes would be helpful in analyzing the drop coalescence in real W/O emulsions.

The major aims of the current study are: (1) To determine the main factors affecting the stability of micrometer water drops, pressed by gravity against large oil-water interface, and (2) To compare the effect of these factors on the stability of the respective water-in-oil emulsions. The effects of the following factors are studied: (i) Drop size between 1 μm and 1 mm; (ii) Surfactant concentration between 10^{-3} wt% and 0.05 wt%; (iii) Viscosity of oil phase, 3 vs. 11 mPa s; (iv) Chain length of the hydrophobic tails of the used surfactants, C12 vs C16. The obtained results are compared, when possible, with the results from our previous study [19] in which we investigated the stability of model oily films with fixed film radius, formed in a capillary cell.

2. Materials and methods

2.1. Materials

In all experiments we used water purified by Milli-Q Organex system (Millipore Inc., USA) to prepare aqueous solutions which contain 150 mM NaCl (≥99.8%, product of Sigma, cat.: 31434). We used *n*-Hexadecane (95%, product of Alfa Aesar, cat.: 43283) and Isopar V (product of Exxon Mobil Corporation, product code: 133639) as oily phases which have dynamic viscosities of 3 and 11 mPa s, and mass densities of 770 and 822 kg m^{-3}, respectively. We studied two nonionic surfactants: Sorbitane monolaurate (Span 20, product of ICI, HLB ≈ 8.6) and Sorbitane monooleate (Span 80, product of Fluka, cat.: 85548, HLB ≈ 4.3) which were dissolved in the oil under stirring on a magnetic stirrer, at room temperature.

2.2. Interfacial tension measurements

To measure the interfacial tension (IFT) of the oil-water interface we used a drop shape analysis on instrument DSA100R and software DSA1 (Krüss GmbH, Germany). The method consists of formation of a pendant water drop on the tip of a needle which is immersed in the oily phase. The software automatically detects the profile of the drop and fits it by Laplace equation of capillarity to determine the interfacial tension, σ.

2.3. Determination of the lifetime of water drops, pressed by gravity against planar oil-water interface

To determine the lifetime of water drops we used the following procedure. In a petri dish with diameter of 3 cm we poured first 1 mL of the water phase (1.4 mm depth), followed by gentle pouring on top of 1.5 mL (2.7 mm depth) of the oily phase with pre-dissolved surfactant. Next, using a needle with diameter varying between 180 and 220 μm, we formed a water drop in the oily phase with different diameters. When the drop fell down to the oil-water interface, a thin emulsion film of type water-oil-water was formed between the drop and the interface, see Fig. 1. We observed the drop on the interface by optical microscope and recorded the lifetime of the drop before it coalesces with the water phase. The drops were released at a distance of 2.5 mm above the level of the oil-water interface. We measured there life time after the moment at which we see the drops in the field of the observation, which is ≈300 μm above the oil-water interface. Before that the drops are not well seen in the observed plane. Therefore, the measured lifetime of the smallest micrometer sized droplets includes the time for their sedimentation to the interface. The latter could be estimated from the known Stokes formula for the velocity of sedimenting spherical

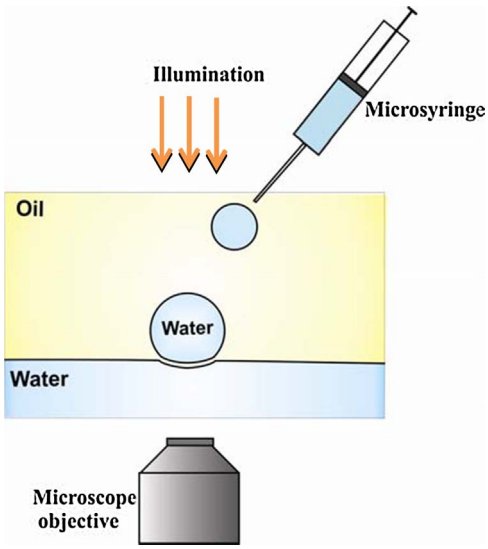

Fig. 1. Schematic presentation of the method for determination of the lifetime of water drops, pressed by gravity against planar oil-water interface by gravity. The water and oil phases are with depths of 1.4 and 2.7 mm, respectively.

particles, $V_{sed} \approx (2\Delta\rho g R^2/9\eta)$ where $\Delta\rho$ is the difference in the mass densities of the two phases, g is the gravity acceleration, R is the drop radius, and η is the viscosity of the continuous (oily) phase. For the larger drops with radius above ca. 50 μm, the sedimentation time has negligible contribution to the measured lifetime.

We performed also experiments by adding not only a single water drop, but several drops with different sizes, pre-formed in an emulsion just before the experiment by mixing the oily and water phases for 20 s by hand, and recorded their lifetime before coalescence. The drops formed by two different methods having the same size show similar life time. Thus, we could build the dependence of the drop lifetime versus drop radius. The precision of drop-size measurement was typically ± 10%, except for the smallest drops with diameter below 10 μm where it was somewhat larger, ± 30%.

In these experiments we used 150 mM NaCl as aqueous phase and Hexadecane or Isopar V with dissolved Span 20 or Span 80 as oily phase. The surfactant concentration was varied between 0.001 and 0.05 wt.%.

2.4. Emulsion stability

Stability against coalescence was studied in water-in-oil emulsions containing 30 vol.% water, with the same oils and surfactant emulsifiers. The surfactants were dissolved in the oily phase, their concentrations were varied between 0.001 and 0.05 wt.%, and 150 mM NaCl was added to the aqueous phase, exactly as in the experiments with single drops. The emulsions were prepared by a two-step procedure. First, coarse emulsion was obtained by slow addition of the water phase into the oily phase under hand stirring. Then this premix was stirred by Ultra Turrax (T25 digital ULTRA-TURRAX, IKA) at 13 500 rpm for 5 min. Afterwards, 100 mL emulsion was placed in a graduated 100 mL cylinder (2.6 mm i.d.) and the time for separation of half of the dispersed water on the cylinder bottom was recorded. For each system, at least 2 independent emulsion samples were prepared to check for reproducibility.

3. Theoretical background

As shown in Refs. [12,17], depending on the size of the drops, they can coalesce with a large interface before or after the formation of a plane-parallel film, if there are no significant repulsive forces between the drop and the oil-water interface.

Let us consider first the so-called “Taylor regime” in which the drops coalesce with the interface before forming a plane-parallel film. The velocity, V_S, of such spherical drops, approaching a large interface, can be presented by the following interpolation formula [12,17]:

$$\frac{1}{V_S} = \frac{1}{V_{TA}} + \frac{1}{V_{St}} \tag{1}$$

Here V_{St} refers to the Stokes formula for the motion of a sphere in an unbounded liquid, while V_{Ta} refers to Taylor formula for the velocity of a sphere approaching a solid surface at a distance, h, which is much smaller than the drop radius, $h << R_d$. The Stokes velocity can be determined from the following expression:

$$V_{St} = \frac{F_d}{6\pi\eta_c R_d} = \frac{2\Delta\rho g}{9\eta_c} R_d^2 \tag{2}$$

where $F_d = \frac{4}{3}\pi R_d^3 \Delta\rho g$ is the gravity force pushing the drops toward the interface, $\Delta\rho$ is the mass density difference between the two fluids, g is gravity acceleration, η_C is viscosity of the continuous phase (the oily phase in our experiments). V_{Ta} can be expressed as:

$$V_{Ta} = \frac{2}{3}\frac{h}{\pi\eta_C R_d^2} F_d \tag{3}$$

where h is the minimum width of the layer between the drop surface and the large interface. After integration of Eqs. (1)–(3) from a certain initial thickness of the oily layer between the drop and the interface, h_{in}, down to the critical thickness at which the drop coalesces with the interface, h_{CR}, the following expression for the drainage time in the case of spherical coalescing drop was obtained [12]:

$$t_S = \frac{9\eta_C}{2\Delta\rho g R_d}\left[\ln\left(\frac{h_{in}}{h_{CR}}\right) + \frac{h_{in} - h_{CR}}{R_d}\right] \tag{4}$$

To apply the above equation, we have assumed $h_{in} \approx 300$ μm and h_{CR} is given by Eq. (8) below.

Let us consider now the bigger water drops, which coalesce after formation of a plane-parallel film with the interface. In this case, the main hydrodynamic resistance is in the plane-parallel film and it is described by Reynolds equation for the velocity of film thinning [12]:

$$V_{Re} = \frac{2F_d h^3}{3\pi\eta_c R_F^4} \tag{5}$$

where $R_F \approx (F_d R_d/\pi\sigma)^{1/2}$ is the radius of the plane-parallel film, which is determined from the force balance on the drop surface. The final expression for the drainage time of drops which form plane-parallel film with the interface before coalescence is given by [12]:

$$t_{Re} = 4.1(\Delta\rho g)^{5/7}\eta_C R_d^{25/7} A_H^{-4/7}\sigma^{-8/7} \tag{6}$$

Here A_H is Hamaker constant and σ is the interfacial tension. Eqs. (4) and (6) were used in Ref. [12] to describe the experimental data for the lifetime of oily drops, pressed by buoyancy against a large oil-water interface at very low protein concentrations in the aqueous solution.

4. Results and discussion

4.1. Interfacial properties of the solutions studied

To characterize the adsorption ability of Span 20 on hexadecane-water interface, we measured the interfacial tension as a function of time, σ(t). The obtained experimental data were fitted by exponential equation and the values of the equilibrium interfacial tension, σ_e, at given concentration was determined from the best fit to the kinetic data. Note that the attempts to describe these data for σ(t) by the equations for diffusion-controlled adsorption [20] gave very poor description – see Fig. S1 in ESI. In contrast, the data description by exponential function which corresponds to barrier-controlled adsorption [20] was much better – see Fig. S1.

The obtained interfacial tension isotherm is compared in Fig. 2 to the isotherm for Span 80, reported in our previous study [19]. These results were fitted by Volmer adsorption isotherm which implies non-localized adsorption with negligible interaction between the adsorbed

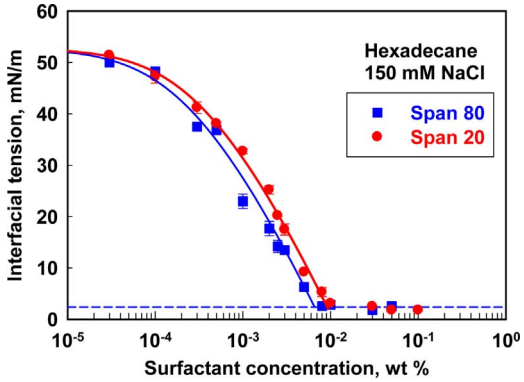

Fig. 2. Interfacial tension on hexadecane-water interface as a function of surfactant concentration for Span 20 (red circles) and Span 80 (blue squares). The continuous curves are the best fits to the experimental data by Volmer equation. (For interpretation of the references to colour in this figure legend, the reader is referred to the web version of this article.)

molecules [20,21]:

$$K_A C_S = \frac{\Gamma}{\Gamma_\infty - \Gamma} \exp\left(\frac{\Gamma}{\Gamma_\infty - \Gamma}\right) \quad (7a)$$

$$\sigma_e = \sigma_0 - kT\Gamma_\infty \ln\left(\frac{\Gamma}{\Gamma_\infty - \Gamma}\right) \quad (7b)$$

Here K_A is the adsorption constant, σ_0 is the surface tension of the pure interface (σ_0 = 52.8 ± 0.2 mN/m for hexadecane-water and Isopar-water interfaces at 20 °C) and Γ_∞ is the maximum surfactant adsorption in the adsorption monolayer. From the values of K_A and Γ_∞ we calculated the adsorption at CMC using Eqs. (7a) and (7b), see Table 1. We use Volmer equation to describe the interfacial tension isotherms, because it is thermodynamically accurate for nonionic surfactants adsorbing on fluid interfaces [20], and brings information about the two most important characteristics of the surfactant molecules: the area-per-molecule at the critical micellar concentration, A_{CMC}, and the surfactant adsorption energy, $\Delta\mu/kT$. From the best fits to the experimental results, shown as continuous curves in Fig. 2, we determined the main adsorption characteristics of Span 20 and Span 80, summarized in Table 1 (see also Ref. [19]). For comparison, we show also in Table 1 the area-per-molecule at CMC, calculated directly from the slope of the curves $\sigma_e(\ln C_s)$, viz from the Gibbs adsorption isotherm. One sees the good agreement between the values calculated from the Volmer and Gibbs isotherms.

The values shown in Table 2 reveal that the characteristics of the Span 20 adsorption layer are very close to those for Span 80 with one important exception. The area per molecule in the Span 20 adsorption layer (0.36 nm^2) is larger by ≈20% than the respective area for Span 80 (0.29 nm^2). This difference indicates a looser packing of the Span 20 molecules in the adsorption layer.

4.2. Determination of the stability of water drops in contact with interface

In Fig. 3, experimental data for the drop lifetime, as a function of drop diameter, are shown by empty red points for water drops, placed in 0.001 wt% Span 80 solution in hexadecane. The obtained results at small drop sizes are more scattered which might be explained with the effect of drop Brownian motion, as shown theoretically by Rojas et al. [22].

To obtain better representation of these experimental data, we divided the results obtained with different drops, in drop-size intervals. For each interval we determined the average drop size and its standard deviation. To represent the lifetime of the drops, falling in the respective interval, we calculated the values of $t_{50\%}$ and $t_{75\%}$ which are defined as the times after which 50% and 75%, respectively of the drops coalesce with the interface. For graphical representation of the experimental data we show $t_{50\%}$ as a mean value, while the difference between $t_{75\%}$ and $t_{50\%}$ is used to characterize the uncertainty in this value. We do not use the average values of the lifetimes and their standard deviations, because we did not determine the real lifetime of the long-living drops, as these drops were observed for up to 300 s only after their placing in the solution. If they live longer, we consider their lifetime as equal to (or bigger than) 300 s.

The comparison between the original experimental data (empty circles) and the statistical values, determined as explained in the preceding paragraph (full squares), are compared in Fig. 3. One sees that we have a very good representation of the original experimental data by the averaged values.

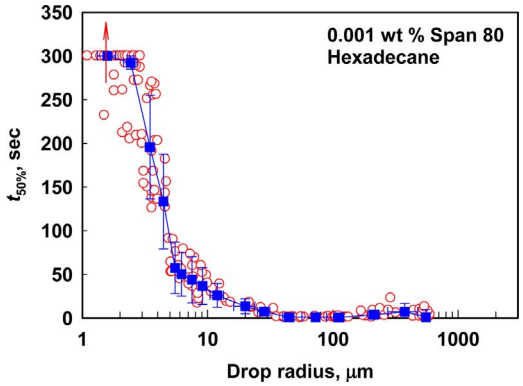

Fig. 3. Original experimental data (empty red circles) and the averaged values of $t_{50\%}$ (blue full squares) for the lifetime of water drops, dispersed in 0.001 wt% Span 80 solution in hexadecane, and pressed by gravity against large oil-water interface (see text for definition of error bars). (For interpretation of the references to colour in this figure legend, the reader is referred to the web version of this article.)

4.2.1. Hydrodynamically stabilized drops

The experimental data for the lifetime for water drops, placed in hexadecane containing 0.001 wt% or 0.003 wt% Span 20 or Span 80, are shown in Fig. 4 as a function of drop diameter. One sees that the lifetime of these drops does not depend on surfactant concentration in this low concentration range, as well as on the type of used surfactant (Span 20 or Span 80). All data lay around one master curve, which consists of three regions: (1) Region 1 for drops with radius R < 20 μm. In this region, the lifetime decreases rapidly with increasing the drop radius. (2) Region 2 for drops with radius between 20 and 100 μm. These drops coalesce within 1–2 s with the large interface and their lifetime does not depend significantly on the drop size at the lower surfactant concentration of 0.001 wt%, whereas the lifetime increases slightly with drop radius at 0.003 wt%, see the full points in Fig. 4. (3) Region 3 for drops with radius above 100 μm, where the lifetime increases very slightly with the drop size and approaches a plateau of ≈10 s for the largest drops.

For most of these large drops, partial coalescence is observed – after breaking of the oily film, formed between the drop and the large interface, fraction of the drop coalesce while smaller drop remains on the interface. This process repeats several times, depending on the size of the initial drop. Similar behavior has been experimentally observed and theoretically described in the literature [23–28]. It was shown that the process of partial coalescence is dynamically driven. It is governed by a competition between the vertical and horizontal forces, appearing upon the collapse of the connected drop [25]. The boundary between partial and total coalescence is characterized by a critical value of the Ohnesorge number which depends on the density and the viscosity ratio of two fluids. However the specific value of the critical Ohnesorge number depends also on the surfactant type and concentration. Therefore, it is difficult to make a direct comparison between our results and the

Table 1
Adsorption constant, K_A, adsorption energy, $\Delta\mu/k_BT$, maximal adsorption, Γ_∞, critical micellization concentration, CMC, area-per-molecule in the adsorption layer at CMC, A_{CMC}, and surface coverage at CMC, $\theta_{CMC} = \Gamma_{CMC}/\Gamma_\infty$, calculated from Volmer equation; and the area-per-molecule at CMC calculated from the Gibbs adsorption isotherm, A_G. The values reported in this table correspond to the total surfactant adsorption. All aqueous solutions contain 150 mM NaCl.

Oily phase	Surfactant	K_A, m^3/mol	$\Delta\mu/kT$	Γ_∞, μmol/m^2	CMC, wt%	A_{CMC}, Å^2	θ_{CMC}	A_G, Å^2
Hexadecane	Span 20	100 ± 40	12.6 ± 0.6	6.5 ± 0.8	0.01	36 ± 3	0.70	32 ± 4
	Span 80	170 ± 40	13.3 ± 0.3	8.4 ± 0.8	0.0065	29 ± 3	0.71	30 ± 3
Isopar V	Span 80	77 ± 40	12.5 ± 0.7	8.9 ± 1.6	0.01	28 ± 5	0.69	29 ± 4

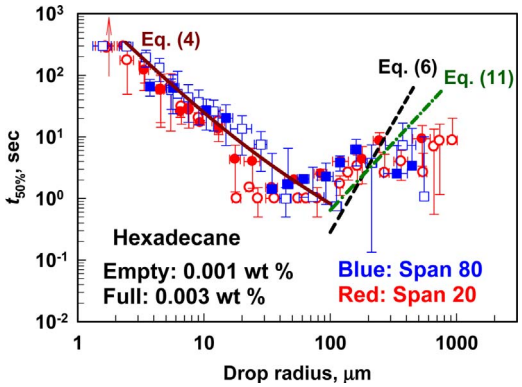

Fig. 4. Lifetime as a function of drop radius for water drops pressed by gravity against hexadecane-water interface in presence of 0.001 wt% (blue squares) or 0.003 wt% (red circles) of Span 20 (empty points) or Span 80 (full points). Water phase contains 150 mM NaCl. Solid continuous curve is calculated by Eq. (4), whereas the dashed curve is calculated according to the second term in Eq. (6). Green dash-dot curve is calculated by Eq. (11) which accounts for the drainage of a film with uneven thickness. (For interpretation of the references to colour in this figure legend, the reader is referred to the web version of this article.)

theoretical predictions for partial coalescence.

In the systems exhibiting partial coalescence, the lifetime of the initial (large drop) is defined till the moment of its coalescence, because it corresponds to the rupture of the oil film, formed between the initial drop and the large interface. The residual smaller drop (formed after a partial coalescence of the larger drop) first bounces from the interface and a new oil film is formed after its sedimentation on the large interface. The lifetime of this newly-formed, smaller drop starts to be measured after its appearance in the field of view of the microscope (focused on the large oil-water interface), because this is the moment of formation of the new oily film between the small drop and the large interface.

Similar dependence for the lifetime vs drop size was reported before for soybean oil drops, placed in aqueous BSA solution [12]. As in our experiments, it was found in [12] that the lifetime of such drops passes through a minimum, as a function of drop diameter.

To compare the experimental data to the theoretical expression, Eq. (4), we should know the initial distance between the droplet and the interface, which in our experiment was around 300 μm, and the critical film thickness for non-deformed drops. To estimate this critical thickness for spherical drops which coalesce before forming a plane-parallel film, we used the estimate proposed by Chesters [29] which presumes that this thickness is reached when the drop capillary pressure, P_C, becomes equal to the Van-der-Waals component of the disjoining pressure Π_{VDW} in the film:

$$\frac{A_H}{6\pi h_{CR}^3} \sim \frac{2\sigma}{R_d} \Rightarrow h_{CR} \approx \left(\frac{A_H R_d}{12\pi\sigma}\right)^{1/3} \tag{8}$$

Substituting h_{CR} from Eq. (8) into Eq. (4) and the values $\eta_C = 3$ mPa s and $\sigma = 40$ mN/m, determined experimentally, we can plot the predictions of Eq. (4) and compare them with the experimental data in Fig. 3. One sees a very good agreement between the experimental data and the theoretical prediction for the drops with radius smaller than ca. 20 μm. Thus, we confirm that these small drops coalesce without forming plane-parallel film and that there are no repulsive forces between the drop and the interface at these very low surfactant concentrations. Note that this is possible, because the surfactant adsorption is rather slow in this range of surfactant concentrations, as seen from the experimental data shown in Fig. S1 in ESI. Therefore, the adsorption layer on the surface of the approaching drop may be still incomplete, due to the limited time for surfactant adsorption after drop formation.

To check further the latter assumptions we calculated the lifetime of larger drops via Eq. (6). The respective theoretical predictions are compared to the experimental data and, as one can see from Fig. 3, Eq. (6) predicts lifetimes which do not agree well with the experimental results for drops with diameter above ca. 100 μm.

One possible explanation for the latter discrepancy could be the fact that the formed films between the drops and the interface are with inhomogeneous thickness. As shown in our previous study [19] the inhomogeneous film thickness leads to faster drainage of the oily films which shortens the lifetime of the studied drops. To account for this effect, we used the equation proposed by Manev et al. [30] for the rate of film thinning which accounts for the non-homogeneous thickness on the rate of film thinning:

$$\frac{V}{V_{RE}} = \sqrt{\frac{(kR_F)^3}{\alpha_1^3}} \tag{9}$$

Here V is the velocity of film thinning for films with inhomogeneous thickness, V_{RE} is given by Eq. (5) above, $\alpha_1 \approx 3.832$ is the first root of the first order Bessel function of the first kind, k is the modulus of the surface wave vector, which for the upper rate limit is given by:

$$k = \sqrt[4]{\frac{24\eta V}{\sigma h^4}} \tag{10}$$

After introducing Eq. (10) into Eq. (9) and using the expressions for the film radius and critical film thickness from Ref. [12], we derived the following equation for the lifetime of larger drops with inhomogeneous film thickness:

$$t_{Inh} \approx 15.3(\Delta\rho g)^{1/5}\eta_C R_d^{11/5} A_H^{-2/5}\sigma^{-4/5} \tag{11}$$

One sees that the dependence of drop lifetime on drop radius is different as compared to Eq. (6). The drainage time increases much more slowly with drop diameter when the films have uneven thickness, as compared to the prediction of Eq. (6). This is illustrated also in Fig. 4 where it is seen that the experimental data for drops with $R_d > 100$ μm are in much better agreement with the prediction of Eq. (11). Still, the experimentally measured lifetime of the largest drops is shorter, as compared to the predicted values by Eq. (11). This shorter lifetime of the largest drops could be due to the fact that the drop surfaces are partially mobile which may lead to even shorter drainage time than the prediction of Eq. (11).

More complex theoretical models are reviewed by Chan et al. in Ref. [31]. These models should be solved numerically, without allowing us to define simple functional dependences on the main system parameters. However, we are particularly interested in finding explicit theoretical expressions for the film lifetime which can be used in a subsequent study (under preparation), aimed to describe the collisions between emulsion droplets during emulsification under dynamic conditions (in turbulent or laminar flow). Eq. (11) is particularly suitable for this purpose, as it is simple explicit expression which describes reasonably well the experimental data for the oil film stability and can be modified to describe the films formed between colliding emulsion drops in dynamic flow.

In the above consideration we do not account also for the possible effect of dynamic adsorption layers with uneven distribution of surfactant molecules along the drop surface (and the related Marangoni stresses) which could appear in the case of drops moving under gravity [32,33]. Such inhomogeneous surfactant distribution could occur in our systems, especially at low surfactant concentrations. However, there is no simple theoretical model to account for this effect and we have refrained from the attempts to include it explicitly in our analysis.

From this series of experiments we conclude that water drops, formed in hexadecane solutions of Span 80 or Span 20 with concentration below the CMC, are hydrodynamically stabilized and their lifetime is equal to the time of film drainage. The small drops coalesce with the interface without forming a plane-parallel film and the drainage time is well described by Eq. (4) which predicts that the drop lifetime decreases with the increase of drop diameter. The larger drops

form plane-parallel film before coalescence and, therefore, their lifetime increases with the drop diameter. However, this increase is much smaller as compared to the predictions of Reynolds equation. That is why we derived a new expression, Eq. (11), for the lifetime of the larger drops which form films with inhomogeneous thickness. The latter expression agrees better with the experimental results but, still, the largest drops coalesce faster, as compared to the theoretical predictions, which is most probably due to the partial mobility of the film surfaces.

4.2.2. Effect of surfactant concentration

In this section we present experimental results about the lifetime of water drops, as a function of drop diameter, for drops formed in hexadecane, containing surfactants of different concentrations. Five surfactant concentrations were studied in the range below and above the CMC. The experimental results for drops, stabilized by Span 20 and Span 80, are compared in Fig. 5. One sees that the stability of water drops stabilized by Span 20 in the concentration range between 0.001 and 0.01 wt% are very similar. As discussed above, these drops are hydrodynamically stabilized. The further increase of Span 20 concentration leads to a significant increase in the stability of both the small and intermediate in size drops, whereas the drops with radius above 100 μm remain very unstable when Span 20 is used, even at concentrations up to 0.05 wt% (viz. at approx. 5 times the CMC, cf. with Table 1).

The behavior of water drops placed in Span 80 hexadecane solutions is different. Even at 0.01 wt% Span 80 (by 50% above the CMC), the stability of the small drops increases significantly. The drops with radius below 30 μm are very stable at this surfactant concentration. However, the bigger drops are again unstable at this concentration, see the blue points in Fig. 5B. Further increase in the concentration of Span 80 leads to very interesting phenomena. The drops with intermediate radii of around 200–300 μm remain very unstable, whereas the smaller and the larger drops are very stable. Therefore, the stability of the drops in this oil solution passes through a very deep minimum, as seen from Fig. 5B.

This minimum in the stability of the drops with intermediated sizes is probably related to the competition of the dynamic processes of surfactant adsorption and film drainage. For drops with size of around 200–300 μm, the drainage time is short and, as a consequence, the drops coalesce with the large interface before forming equilibrium adsorption layer on their surface [19]. In contrast, the drainage time is longer than the adsorption time for bigger drops, which allows the formation of a dense adsorption layer on the film surfaces, able to stabilize the drops by steric repulsion.

4.2.3. Effect of the oily phase

In the current section we compare the lifetime of water drops placed in Span 80 solutions in hexadecane or Isopar, at different Span concentrations, see Fig. 6.

For hydrodynamically stabilized drops, at a concentration 3-times lower than the CMC, the experimental data are well described by Eq. (4) for the Taylor regime. Also, the stability of water drops in Isopar is higher as compared to hexadecane, due to the higher Isopar viscosity. These results confirm that, at low surfactant concentrations, the drop stability is determined entirely by the drainage time required to reach the critical thickness for film rupture.

At surfactant concentrations close to the CMC, we observe similar behavior for hexadecane and Isopar. The small drops become very stable, whereas the big drops remain very unstable and their life time is around 10 s only. The threshold drop diameter above which the drops become unstable is smaller for the drops placed in Isopar, as compared to hexadecane, see Fig. 6B. The latter difference is probably related to the fact that this surfactant concentration, 0.01 wt%, is very close to CMC for Isopar while it is around 1.5 times higher than the CMC for hexadecane, as shown in our previous study [19].

At 0.05 wt% Span 80, the stability of the water drops passes through a minimum, as a function of drop radius, in both Isopar and hexadecane.

Therefore, we conclude that the increase of the viscosity of the continuous phase leads to a significant increase in the stability of the hydrodynamically stabilized drops, at concentrations below CMC. In addition, the worse packing of Span 80 molecules within the adsorption layers formed on Isopar-water interface, as compared to hexadecane-water interface [19], leads to lower stability of the water drops at concentrations around and above the CMC.

4.3. Stability of batch emulsions

To characterize the stability of batch W/O emulsions we used the experimental procedure described in Section 2.4. The experimental conditions were the same as those in the single-drop experiments, described above (except for the hydrodynamic conditions).

The obtained results for the time needed to separate half of the emulsified water, are shown in Fig. 7. One sees that the stability of emulsions, prepared at concentrations below CMC, is very low for both oils, Isopar and hexadecane, as well as for both emulsifiers, Span 20 and Span 80. At Span concentrations around the CMC (0.01 wt%) the stability is higher for emulsions stabilized by Span 80, as compared to Span 20, which is in a very good agreement with the results obtained with single drops. Moreover, the stability of hexadecane emulsions is higher as compared to Isopar emulsions at this concentration, which can be explained with the different packing of the surfactant molecules in the respective adsorption layers (worse for Isopar as compared to hexadecane [19]). This effect disappears at higher surfactant concentrations where the stability of both hexadecane and Isopar V emulsions is very high for Span 80 solutions. On the other hand, when Span 20 is used as emulsifier, the emulsion stability is very low and fast separation of the water phase is observed, even at high surfactant concentrations (5 times above the CMC). This effect correlates very well to the observed low stability of the water drops with intermediate and large diameter when Span 20 is used as emulsifier.

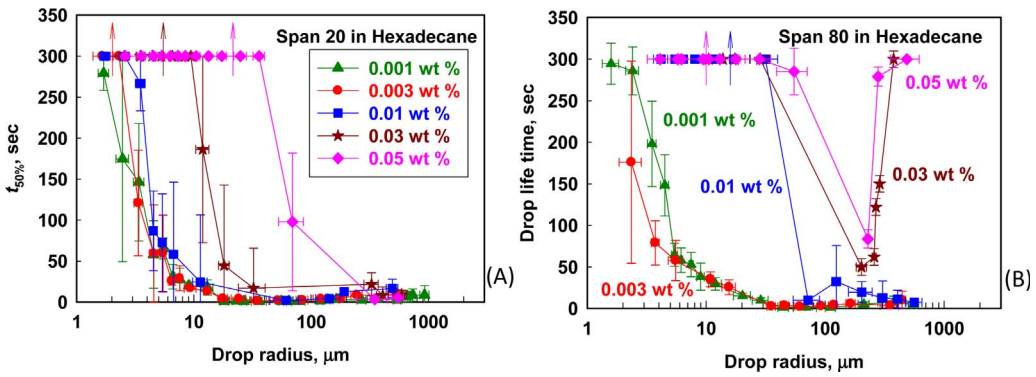

Fig. 5. Drop life time as a function of drop radius for water drops in hexadecane, pressed by gravity against large oil-water interface and stabilized by (A) Span 20 or (B) Span 80 with different concentrations, as indicated in the figures.

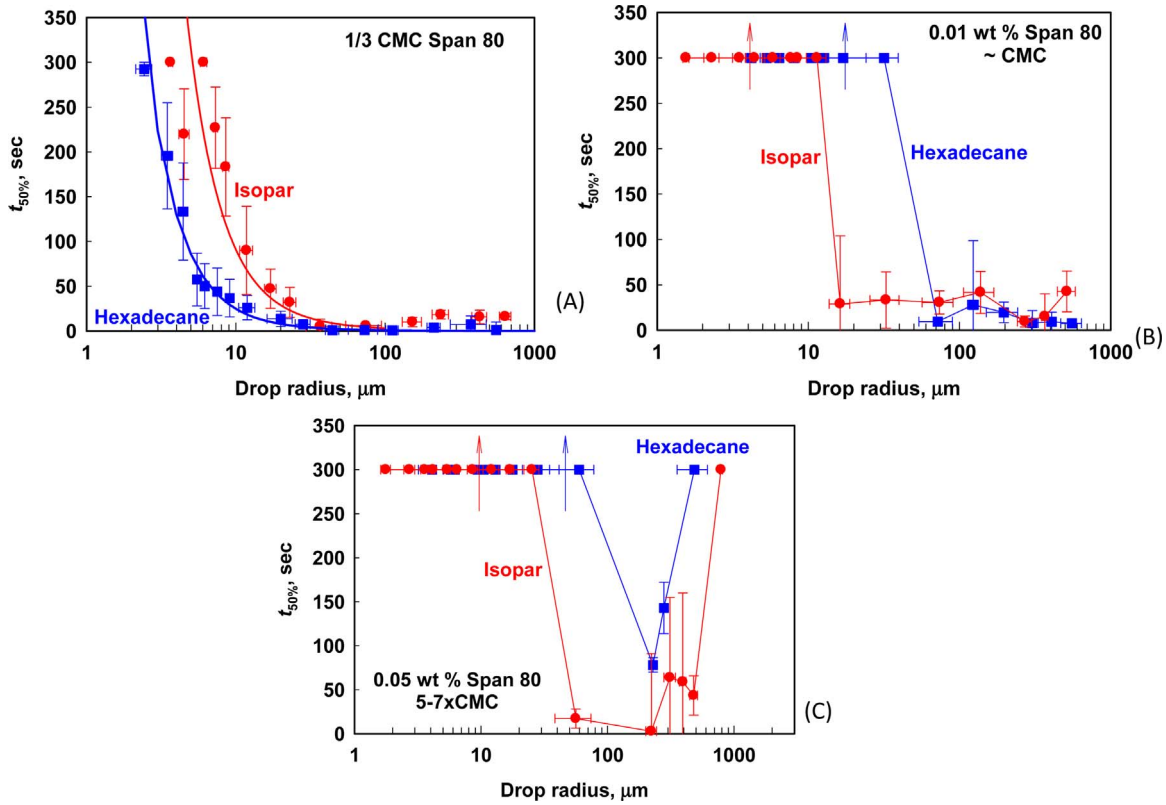

Fig. 6. Median drop lifetime, as a function of drop radius, for water drops stabilized by Span 80 of different concentrations: (A) 1/3 CMC; (B) 0.01 wt% and (C) 0.05 wt% in hexadecane (blue squares) or Isopar V (red circles). (For interpretation of the references to colour in this figure legend, the reader is referred to the web version of this article.)

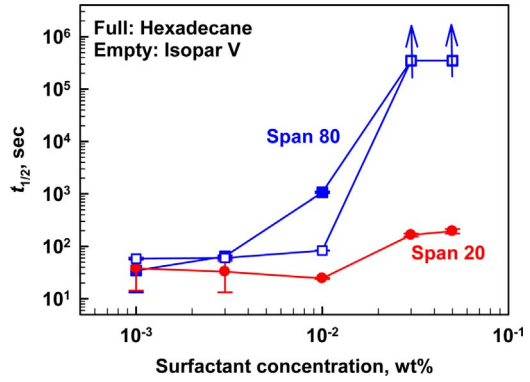

Fig. 7. Deemulsification time, as a function of surfactant concentration, for water-in-hexadecane emulsions (full symbols) and water-in-Isopar V emulsions (empty symbols), stabilized by Span 20 (red circles) or Span 80 (blue squares). (For interpretation of the references to colour in this figure legend, the reader is referred to the web version of this article.)

5. Summary and conclusions

Systematic series of experiments are performed to characterize the stability of water drops, as a function of their size, surfactant concentration, surfactant chain length, and viscosity of the oily phase. The main results and conclusions could be summarized as follows:

The water drops placed in Span solutions with concentrations below the CMC are hydrodynamically stabilized – their lifetime is determined exclusively by the time required for thinning of the oily layer, formed between the approaching drop and the large oil-water interface. In this concentration range, the drop stability passes through a minimum when increasing the drop diameter. Also, the experimental results for the small drops are described very well by theoretical expressions, whereas the lifetimes of the bigger drops are shorter than the theoretical predictions, due to two effects – the uneven thickness of the thinning film and the partial mobility of the film surfaces. In this concentration range, the increase of solution viscosity enhances the drop stability. There is no significant difference between the lifetimes of the water drops, stabilized by Span 20 and Span 80, in this low concentration range.

At concentrations around the CMC, the stability of the drops smaller than ca. 20 μm, increases strongly for both surfactants and oils studied, whereas the stability of the big drops remains very low.

At concentrations above the CMC, the stability of the water drops in hexadecane or in Isopar V solutions passes through a minimum – the big and the small drops are very stable, whereas the drops with intermediate radius of ca. 200 μm are unstable when Span 80 is used as emulsifier. For water drops placed in Span 20, the big drops are unstable even at high surfactant concentration (5 times the CMC). The lower stability of water drops in such solutions of Span 20 is explained with the looser packing of the surfactant molecules within the respective adsorption layers, as revealed from the area-per-molecule (see Table 1), determined from the surface tension isotherm of Span 20.

The observed low stability of the bigger drops in Span 20 solutions has significant impact on the stability of the respective batch emulsions which undergo much faster phase separation, as compared to emulsions stabilized by Span 80.

In general, very good agreement is observed between the stability of batch water-in-oil emulsions and the stability of the single water drops in the model experiments. Therefore, these results shed light on the effect of several important emulsification factors, such as surfactant concentration and drop size, on the outcome of the emulsification experiments and on the stability of the obtained water-in-oil emulsions.

On the other hand, the analysis of the dynamic effects during emulsification in turbulent flow requires much more elaborated approach which can be developed using information from the current study about the film lifetime between colliding drops. We note that the

drops in the agitated emulsions could be also out-of-equilibrium with the surfactant solution (as the single drops at low surfactant concentrations in our experiments), because the drop breakage during emulsification creates a new interface and there is a finite time before this freshly-born interface is covered with surfactant adsorption layer [33–35].

Acknowledgments

The authors are especially grateful to Mrs. Mila Temelska (Sofia University) for measuring interfacial tension isotherm of Span 20. The authors gratefully acknowledge the support of this study by BASF. This work is closely related to the activity of COST MP 1305 “Flowing matter”.

References

[1] E.G. Cockbain, T.S. McRoberts, The stability of elementary emulsion drops and emulsions, J. Colloid Sci. 8 (1953) 440–451.
[2] T. Gillespie, E.K. Rideal, The coalescence of drops at an oil-water interface, Trans. Faraday Soc. 52 (1956) 173–183.
[3] G.A.H. Elton, R.G. Picknett, The coalescence of aqueous droplets with an oil/water interface, Butterworths, London, Proceedings of the 2nd International Congress of Surface Activity vol. 1, (1957) 288.
[4] L.E. Nielsen, R. Wall, G. Adams, The coalescence of liquid drops at oil-water interfaces, J. Colloid Sci. 13 (1958) 441–458.
[5] G.E. Charles, S.G. Mason, The coalescence of drop with flat liquid/liquid interfaces, J. Colloid Sci. 15 (3) (1960) 236–267.
[6] S. Hartland, The coalescence of a liquid drop at a liquid–liquid interface. Part I: drop shape, Trans. Inst. Chem. Eng. 45 (1967) 97–101.
[7] S. Hartland, The coalescence of a liquid drop at a liquid–liquid interface. Part III: film rupture, Trans. Inst. Chem. Eng. 45 (1967) 109–114.
[8] S. Hartland, The coalescence of a liquid drop at a liquid–liquid interface. Part V: the effect of surface active agents, Trans. Inst. Chem. Eng. 46 (1968) 275–282.
[9] T.D. Hodgson, J.C. Lee, The effect of surfactants on the coalescence of a drop at an interface I, J. Colloid Interface Sci. 30 (1) (1969) 94–108.
[10] K.A. Burill, D.R. Woods, Film shapes for deformable drops at liquid–liquid interfaces. III. Drop rest-times, J. Colloid Interface Sci. 42 (1973) 35–51.
[11] E. Dickinson, B.S. Murray, G. Stainsby, Coalescence stability of emulsion-sized droplets at a planar oil–water interface and the relationship to protein film surface rheology, J. Chem. Soc. Faraday Trans. 84 (1988) 871–883.
[12] E.S. Basheva, T.D. Gurkov, I.B. Ivanov, G.B. Bantchev, B. Campbell, R.P. Borwankar, Size dependence of the stability of emulsion drops pressed against a large interface, Langmuir 15 (1999) 6764–6769.
[13] P. Ghosh, Coalescence of bubbles in liquid, Bubble Sci. Eng. Technol. 1 (2009) 75–87.
[14] S. Samanta, P. Ghosh, Coalescence of bubbles and stability of foams in Brij surfactant systems, Ind. Eng. Chem. Res. 50 (2011) 4484–4493.
[15] S. Samanta, P. Ghosh, Coalescence of bubbles and stability of foams in aqueous solutions of Tween surfactants, Chem. Eng. Res. Des. 89 (2011) 2344–2355.
[16] G. Suryanarayana, P. Ghosh, Adsorption and coalescence in mixed-surfactant systems: air-water interface, Ind. Eng. Chem. Res. 49 (2010) 1711–1724.
[17] I.B. Ivanov, P.A. Kralchevsky, Stability of emulsions under equilibrium and dynamic conditions, Colloids Surf. A 128 (1997) 155–175.
[18] E. de Malmazet, F. Risso, O. Masbernat, V. Pauchard, Coalescence of contaminated water drops at an oil/water interface: influence of micro-particles, Colloids Surf. A: Physicochem. Eng. Aspects 482 (2015) 514–528.
[19] N. Politova, S. Tcholakova, N.D. Denkov, Factors affecting the stability of water-oil-water emulsion films, Colloids Surf. A: Physicochem. Eng. Aspects 522 (2017) 608–620.
[20] P.A. Kralchevsky, K.D. Danov, N.D. Denkov, Chemical physics of colloid systems and interfaces, in: K.S. Birdi (Ed.), Handbook of Surface and Colloid Chemistry, CRC Press, New York, 2008.
[21] A.W. Adamson, A.P. Gast, Physical Chemistry of Surfaces, sixth ed., Wiley, New York, 1997.
[22] C. Rojas, M. Garcia-Sucre, G. Urbina-Villalba, Lifetime of oil drops pressed by buoyancy against a planar surface: large drops, Phys. Rev. E 82 (2010) 056317.
[23] G.E. Charles, S.G. Mason, The mechanism of partial coalescence of liquid drops at liquid/liquid interfaces, J. Colloid Sci. 15 (1960) 105–122.
[24] S.T. Thoroddsen, K. Takehara, The coalescence cascade of a drop, Phys. Fluids 12 (2000) 1265–1267.
[25] F. Blanchette, T. Bigioni, Partial coalescence of drops at liquid interfaces, Nat. Phys. 2 (2006) 254–257.
[26] T. Gilet, N. Vandewalle, S. Dorbolo, Controlling the partial coalescence of a droplet on a vertically vibrated bath, Phys. Rev. E 76 (2007) 035302-1–035302-4.
[27] X. Chen, S. Mandre, J.J. Feng, Partial coalescence between a drop and a liquid–liquid interface, Phys. Fluids 18 (2006) 051705-1–051705-4.
[28] F. Blanchette, L. Messio, J.W.M. Bush, The influence of surface tension gradients on drop coalescence, Phys. Fluids 21 (2009) 072107-1–072107-9.
[29] A.K. Chesters, Modelling of coalescence processes in fluid-liquid dispersions: a review of current understanding, Chem. Eng. Res. Des. 69 (1991) 259.
[30] E. Manev, R. Tsekov, R.B. Radoev, Effect of thickness non-homogeneity on the kinetic behavior of microscopic foam film, J. Dispers. Sci. Technol. 18 (1997) 769–788.
[31] D.Y.C. Chan, E. Klaseboer, R. Manica, Film drainage and coalescence between deformable drops and bubbles, Soft Matter 7 (2011) 2235–2264.
[32] K.J. Stebe, S.-Y. Lin, C. Maldarelli, Remobilizing surfactant retarded fluid particle interfaces. I. Stress-free conditions at the interfaces of micellar solutions of surfactants with fast sorption kinetics, Phys. Fluids A 3 (1991) 3–20.
[33] V.G. Levich, Physicochemical Hydrodynamics, Prentice Hall, Englewood Cliffs, New Jersey, 1962.
[34] P. Walstra, Formation of emulsions, Encyclopedia of Emulsion Technology, Marcel Dekker, New York, 1983 Chapter 2.
[35] S. Tcholakova, N. Denkov, A. Lips, Comparison of solid particles, globular proteins and surfactants as emulsifiers, Phys. Chem. Chem. Phys. 10 (2008) 1608–1627.